SAND99-1139J

PERMEABILITY UPSCALING MEASURED ON A BLOCK OF BEREA SANDSTONE: RESULTS AND INTERPRETATION

Vincent C. Tidwell
Sandia National Laboratories
Geohydrology Department
Albuquerque, New Mexico

John L. Wilson
New Mexico Inst. of Mining & Technology
Dept. of Earth & Environmental Sciences
Socorro, New Mexico

To physically investigate permeability upscaling over 13,000 permeability values were measured with four different sample supports (i.e., sample volumes) on a block of Berea Sandstone. At each sample support spatially-exhaustive permeability data sets were measured, subject to consistent flow geometry and boundary conditions, with a specially adapted minipermeameter test system. Here, we present and analyze a subset of the data consisting of 2304 permeability values collected from a single block face oriented normal to stratification. Results reveal a number of distinct and consistent trends (i.e., upscaling) relating changes in key summary statistics to an increasing sample support. Examples include the sample mean and semivariogram range that increase with increasing sample support and the sample variance that decreases. To help interpret the measured mean upscaling we compared it to theoretical models that are only available for somewhat different flow geometries. The comparison suggests that the non-uniform flow imposed by the minipermeameter coupled with permeability anisotropy at the scale of the local support (i.e., smallest sample support for which data is available) are the primary controls on the measured upscaling. This work demonstrates, experimentally, that it is not always appropriate to treat the local-support permeability as an intrinsic feature of the porous medium; that is, independent of its conditions of measurement.

KEY WORDS: permeability, upscaling, Berea Sandstone, minipermeameter, non-uniform flow, local-scale processes

INTRODUCTION

Rarely can permeability data be acquired at the desired scale of analysis. The resulting disparity between the scale at which permeability data are measured and the desired scale of analysis, which is almost always larger than the former, necessitates the application of averaging or upscaling models. Because upscaling confronts a wide range of simulation and prediction problems in the geosciences, a variety of analytical and numerical models have been developed. As a full deterministic description of natural geologic materials is impractical, upscaling is commonly approached though stochastic means with the spatially heterogeneous qualities of the porous media treated as correlated random variables. Upscaling is accomplished by spatially integrating the stochastic partial-differential equations derived from the fundamental conservation laws of continuum mechanics. The roots of permeability upscaling lie at the pore scale and hence significant effort has been made to predict the macroscopic permeability from the pore-scale characteristics of the porous medium (e.g., Marle, 1967; Cushman, 1984; Bear and Bachmat, 1990). This level of upscaling is generally averted due to the availability of permeability data measured on some macroscopic sample support (i.e., sample volume). Upscaling of permeability values from the measurement scale to the desired scale of analysis is conditioned on the spatial statistical characteristics of the permeability. Where simplifying assumptions concerning the spatial structure of the porous medium can be made and flows are uniform, upscaled permeability estimates are derived directly through analytical solutions (e.g., Gutjahr et al., 1978, Dagan, 1981; Gelhar and Axness, 1983; Deutsch, 1989; Rubin and Gomez-Hernandez, 1990; Desbarats, 1992a). Where non-uniform flows are encountered a single effective permeability value can no longer be defined that is dependent solely on the statistical properties of the permeability; rather, upscaling must explicitly account for the flow conditions unique to the problem (e.g., Matheron, 1967; Ababou and Wood, 1990; Desbarats, 1992b; Neuman and Orr, 1993; Indelman and Abramovich, 1994; Sanchez-Vila, 1997). For cases involving complicated heterogeneities and/or flows numerical solutions to the upscaling problem are necessitated (e.g., White and Horne, 1987;

Kitanidis, 1990; Kossack et al., 1990; Durlofsky, 1991). The key assumption of these stochastic theories is that the permeability is a weakly stationary or periodic, ergodic random variable. Where the permeability exhibits long-range spatial persistence, fractal (e.g., Neuman 1994) theories have been proposed for quantifying upscaling behavior. Although such theoretical and numerical studies add greatly to our understanding of permeability upscaling, physical data collected under carefully controlled conditions are needed to suggest and test models.

Laboratory upscaling experiments have recently been conducted on a block of Berea Sandstone. These studies were made possible by a unique minipermeameter test system (Tidwell and Wilson, 1997) that we call the Multi-Support Permeameter (MSP). Here, we present 2,304 permeability values measured on a single block face of the Berea Sandstone sample. These permeability data were measured with four different sample supports spanning 2.5 orders of magnitude on a per-volume basis. Although the Berea Sandstone is known for its relatively uniform permeability characteristics, distinct and consistent upscaling trends were measured. The measured upscaling in the mean permeability is compared with that predicted by theoretical models that differ according to their assumptions concerning flow uniformity. These comparisons are used to interpret the data and to infer the physical controls on the measured permeability upscaling.

METHODS

To physically investigate permeability upscaling, extensive data sets are collected over a series of discrete sample supports. Key attributes of the data include: 1) all measurements, regardless of sample support, are made subject to consistent boundary conditions and the same flow geometry; 2) measurements are non-destructive thus allowing all data to be collected from the same physical sample; 3) dense sampling grids are employed to provide detailed spatial information on the permeability field; and, 4) measurements are precise, subject to small and consistent measurement error. By acquiring data in this manner, sampling artifacts that can aggravate quantification of permeability upscaling are minimized or eliminated.

Collection of such permeability data is made possible with a specially adapted minipermeameter test system, which we call the Multi-Support Permeameter (MSP) (Tidwell and Wilson, 1997). Permeability data are acquired with this system by simply compressing a tip seal against a flat, fresh rock surface while injecting gas at a constant pressure. Using information on the seal geometry, gas flow rate, gas injection pressure, and barometric pressure, the permeability is calculated using a modified form of Darcy's Law (Goggin et al., 1988). Automation of this process is achieved by coupling a minipermeameter with an x-y positioner and computer control system. The minipermeameter functions as the measurement device of the MSP and consists of four electronic mass-flow meters (0-50, 0-500, 0-2000, and 0-20,000 cm^3/min. at standard conditions), a pressure transducer (0-100 kPa gauge), a barometer, and a gas temperature sensor that are all connected to a regulated source of compressed nitrogen. Measurements are made according to a user specified sampling grid programmed into the x-y positioner. Along with locating the tip seal for sampling, the positioner also compresses the tip seal squarely against the rock surface with a consistent and constant force. The minipermeameter and x-y positioner are configured with a computer control system to govern the data acquisition process and provide unattended operation of the MSP. A full description and analysis of the MSP is given by Tidwell and Wilson (1997).

Measurements are made at different sample supports, subject to consistent boundary conditions and flow geometries, by simply varying the radius of the tip seal. Tip seals, specifically designed for this program, consist of a rigid aluminum housing to which a molded silicone rubber ring is affixed. A series of such tip seals have been built with inner radii r_i of 0.15, 0.31, 0.63, and 1.27 cm and an outer radii (r_o) measuring twice the inner. Critical to precise measurement is a consistent and known tip seal geometry under compressed conditions. For this reason, each of the tip seals is equipped with an internal spring-driven guide to maintain a constant inner seal diameter. For the 0.63 cm and smaller tip seals, which experience considerable deformation on compression, an immobile outer guide is also employed.

The ring-shaped tip seal of the minipermeameter imposes a strongly divergent flow geometry during testing. The non-uniform flow geometry raises questions concerning what is actually measured by tip seals of different size. To help with this, linear filter theory was employed to analyze a series of data sets measured with different size tip seals on the Berea Sandstone sample (Tidwell et al., 1999). Weighting (filter) functions were calculated from the data that provide insight into both the effective size of the sample support (i.e., sample volume), as well as how the instrument spatially weights the heterogeneities comprising that support. Results suggest that the characteristics and behavior of the calculated weighting functions are consistent with the basic physics governing gas flow from a minipermeameter tip seal. The calculated weighting functions are centered on the measurement, consistent with the symmetry of the minipermeameter tip seal. Each weighting functions decays according to a nonlinear function of radial distance, consistent with the divergent flow geometry imposed by the minipermeameter. Although the Berea Sandstone exhibits an anisotropic permeability distribution (see below) it was difficult to discern such characteristics in the calculated weighting functions. Consequently, we currently conceptualize the MSP flow field as a hemisphere with effective radius, r_{eff},which is defined as the radius where the weighting function is effectively zero. The weighting functions also change in a predictable manner as the tip seal size is varied. Specifically, as the tip seal size becomes larger r_{eff} of the measurement increases. Although additional work is needed to fully quantify the sample support associated with each tip seal, we and others (e.g., Goggin et al., 1988) believe that r_{eff} is roughly proportional to r_i, hence the sample support increases by a power of 8 for each doubling of r_i.

The non-uniform flow geometry imposed by the minipermeameter tip seal also influences the measured permeability upscaling. Although many hydraulic testing methods (e.g., pump tests, tracer tests, slug tests) are subject to non-uniform flow, relatively little theoretical work has been devoted to upscaling under such conditions. In fact, no upscaling studies have been conducted to date for flow geometries consistent with that of the minipermeameter. Thus, we do not test existing theories, but rather examine the results in light of these theories.

RESULTS

Permeability data were acquired from a 0.3 by 0.3 by 0.3 m block of Berea Sandstone obtained from Cleveland Quarries in Amherst, Ohio. The Berea Sandstone is believed to be of Mississippian Age with its origins in a low-energy, fluvial-deltaic environment (Pepper et al., 1954). According to visual inspection (Figure 1a), the sample may be characterized as a very-fine grained, well sorted quartz sandstone. The sample is relatively featureless except for faint subhorizontal stratification. The Berea Sandstone was selected for testing because of its common use in laboratory studies and its relatively simple physical features. In short, it is one of the most uniform (deterministically homogeneous) rock samples we've encountered. Samples from other depositional environments, with much larger permeability variances and different spatial correlation structures, have likewise been investigated and are reported elsewhere (Tidwell and Wilson, 1999a; 1999b).

Over 13,000 permeability measurements were collected over all six faces of the sandstone sample; however, the analyses reported here focus on 2304 data collected from a single face cut normal to the stratification (which we term Face 3). Measurements were made on the exact same grid using the 0.15, 0.31, 0.63, and 1.27 cm r_i tip seals. Although larger tip seals were available for sampling they were not used because of the limited dimensions of the rock sample. The sampling grid contained 576 measurement points organized on a square 24 by 24 lattice on 0.85

cm centers. To avoid boundary effects on the measurements, a total grid size of 19.5 by 19.5 cm was used that provides a 5.25 cm buffer between the grid and edge of the block.

Spatial Permeability Measurements

The natural-log permeability fields (i.e., $\ln[k(x,z)]$ where k is permeability in m^2, and x and z denote the spatial location) measured with the 0.15, 0.31, 0.63, and 1.27 cm r_i tip seals are given in Figure 1. Three important attributes of these permeability fields should be noted. First, comparisons drawn between the photograph (Figure 1a) and permeability fields reveal that the stratification faintly visible to the eye in the Berea Sandstone correlates with the anisotropy exhibited by the permeability fields. Second, each of the four tip seals reproduce the same basic spatial permeability patterns. Specifically, laminae of alternating "high" and "low" permeability are located in the same position in each of the data sets (e.g., the low-permeability laminae centered at z=7.5 cm, and at 18.5 cm). In fact, these laminae can be traced across all four block faces cut normal to the stratification (Tidwell and Wilson, 1997; Tidwell et al., 1999). Finally, distinct smoothing of the permeability field is evident as the tip seal size increases. This smoothing occurs because measurements made at larger supports interrogate more rock and hence average over more spatial variability than do measurements made at smaller sample supports.

The cumulative distribution functions (CDFs) for the natural-log permeability data measured with each of the four tip seals are given in Figure 2 while the corresponding summary statistics are given in Table 1. The CDFs are characterized by a small range and correspondingly low variance. The natural-log permeability data for the 0.15 cm tip seal are approximately normally distributed; however, as the tip seal size increases, asymmetry in the distribution becomes more apparent. Several distinct trends with changing sample support are evident. The sample mean increases with increasing sample support while the sample variance decreases. Inspection of the CDFs reveals that upscaling influences the distribution beyond the sample mean and variance, as evidenced by the increasing asymmetry of the distribution and the distinct difference in the degree of upscaling exhibited by the upper and lower tails of the CDFs.

To investigate the spatial correlation of the permeability data, full two-dimensional semivariograms were calculated for each of the natural-log permeability data sets using Fourier analysis (via Fast Fourier Transforms, see Bracewell, 1986; Tidwell et al., 1999). The two-dimensional semivariogram calculated for the 1.27 cm data set is given in Figure 3 revealing anisotropy in the permeability field. Transects oriented along the major and minor permeability axes are plotted in Figure 4. The transects show strong spatial correlation parallel to the stratification, as exhibited by a range that extends beyond the length of the semivariogram (Figure 4a), and very weak correlation in the orthogonal direction (Figure 4b). A weak hole-effect is apparent normal to stratification reflecting the layered (i.e., periodic) structure of the Berea Sandstone (Figure 1).

The sample semivariograms calculated from the four different tip seal data sets have been fit with an exponential γ_i model

$$\gamma_i(\vec{s}) = C_i + \sigma_i^2\left(1 - \exp\left[-\frac{3\vec{s}}{\vec{\lambda}_i}\right]\right) \tag{1}$$

where C_i is the nugget, σ_i^2 the variance of the natural-log permeability, $\vec{\lambda}_i = (\lambda_{x,i}, \lambda_{z,i})$ the semivariogram range vector (cm), and $\vec{s} = (s_x, s_z)$ the separation vector (cm) in the principal directions (see Figure 1). The subscript i designates the tip seal data set to which the semivariogram model is fit. Model parameters fit to the semivariogram data are given in Table 2. The coefficients for the exponential model oriented parallel to stratification should be viewed with caution as the length of the sample semivariogram is insufficient to uniquely estimate the range and sill parameters. Nevertheless, a number of consistent and distinct trends are evident among the semivariograms. First, the sill of the semivariogram decreases with increasing sample support, consistent with the decreasing variance, while the general shape of the semivariogram remains unchanged (except for dampening of the hole-effect in Figure 4b). Also, the fitted range values $\vec{\lambda}_i$ increase linearly with sample support reflecting the linear increase in tip seal radius (Clark, 1977; Journel and Huijbregts, 1978).

As noted above, all six faces of the Berea Sandstone sample were investigated. Although there would be some advantage to presenting this data all in one place, the logistics of conveying this extensive set of information in a concise manner is a formidable task. As all six faces exhibit very similar upscaling characteristics it would be redundant for purposes of this paper to present the other faces here. However, data beyond that provided above, can be found in other references. Tidwell and Wilson (1997) present data taken from Face 5, which is located directly opposite of the block from Face 3 (given here), while data from Face 2, orthogonal to Faces 3 and 5 and oriented normal to stratification, can be found in Tidwell et al. (1999). Each sampled block face exhibits a roughly log-normal permeability distribution with a mean that increases with increasing sample support and a variance that decreases. In each case the semivariogram exhibits an exponential structure with a range that extends beyond the length of the semivariogram parallel to stratification and much shorter-range correlation normal to stratification. With increasing sample support, the magnitude of the semivariogram always decreases, the range increases, while the general anisotropic exponential spatial structure is maintained. The most noteworthy differences among block faces are in the absolute magnitudes of the mean and variances of the log permeabilities. Mean permeabilities may vary by a full natural-log unit (for a given tip seal size) while variances may differ by as much as a factor of 3.

Model Comparison

We now interpret the measured permeability upscaling through comparison with theoretical upscaling models. Although there are a number of interesting upscaling trends evident in the data, we limit our attention to the sample mean. We draw comparison with two different analytical models, one that assumes uniform-flow conditions and another that assumes non-uniform radial flow. We recognize that these models are not fully consistent with the experimental conditions, but there are no published analytical or numerical studies that deal with permeability upscaling for hemispherical flow in an anisotropic medium. The development of such theories are well beyond the scope of the current paper. For this reason, our intent is not to test the theories but use them as limiting cases to interpret the key processes governing the measured upscaling. A careful review of the fundamental modeling assumptions in light of actual experimental conditions forms the basis of our analysis.

The sample means calculated from the Berea Sandstone data measured on Face 3 with the four different-size tip seals are plotted in Figure 5 as a function of the inner tip seal radius. For this analysis we have plotted the arithmetically averaged mean permeabilities ($\bar{k}_i^a = E[k_i(\vec{x})]$, where i designates tip seal size). Inspection of Figure 5 reveals that the sample mean follows a smooth trend, increasing by a factor of 1.5 for a 2.5 order of magnitude increase in sample support.

Our first comparison is drawn with an effective permeability model that assumes an infinite domain (i.e., the domain size is much larger than the correlation length scales of the medium, $\bar{\lambda}_o$) and mean uniform-flow conditions. Our permeability measurements are clearly inconsistent with the modeling assumptions; nevertheless, we perform this analysis so that we may compare results with the test case assuming non-uniform flow. We make our comparison with the spectral/perturbation model of Gelhar and Axness (1983). Their model can be tailored to our problem by considering the MSP flow geometry and the spatial structure of the Berea Sandstone.

Given the orientation of the MSP on this face of the rock, normal to stratification, we assume that flow parallel to stratification dominates. According to Gelhar and Axness, the effective permeability, $\bar{k}_{xx}$, of an infinite domain subject to uniform flow oriented parallel to stratification is

$$\bar{k}_{xx} = \bar{k}_o^g \exp\left[\sigma_o^2\left(\frac{1}{2} - g_{xx}\right)\right] \tag{2}$$

where $\bar{k}_o^g$ is the geometric mean $\left(\bar{k}_o^g = \exp\left(E\left[\ln\left(k_o(\vec{x})\right)\right]\right)\right)$ of the point-support permeability, k_o (i.e., associated with an infinitely small sample volume), σ_o^2 is the corresponding variance $\left(\sigma_o^2 = Var\left[\ln\left(k_o(\vec{x})\right)\right]\right)$, and g_{xx} is a constant accounting for the spatial anisotropy of the natural-log permeability field. Although we do not have exact measures of the correlation length scales for this medium, $\vec{\lambda}_o$ (as determined from k_o), we do know that $\vec{\lambda}_o$ is slightly smaller than the semivariogram range values determined from the smallest, 0.15 cm, tip seal data set (Clark, 1977; Journel and Huijbregts, 1978). From the semivariograms (Figure 4) and inspection of the sampled block face it is clear that the correlation length scale parallel to stratification is much larger than that normal to stratification. For this case we find $g_{xx} \cong 0$ from Figure 4 of Gelhar and Axness (1983). Note that for $g_{xx} = 0$ the right-hand-side of Equation 2 is simply the arithmetic average of $k_o(\vec{x})$, which is a reasonable result considering our assumption of uniform flow oriented parallel to stratification.

As $\bar{k}_o^g$ and σ_o^2 (which are associated with the point support) have not been measured, a direct calculation of $\bar{k}_{xx}$ is not possible. However, we can expect that the mean permeability measured with the largest tip seal $\bar{k}_{1.27}^g$ to be less than or equal to $\bar{k}_{xx}$ and likewise $\bar{k}_o^g \leq \bar{k}_{0.15}^g$. Thus, we can write

$$\frac{\bar{k}^{g}_{1.27}}{\bar{k}^{g}_{0.15}} \le \frac{\bar{k}_{xx}}{\bar{k}^{g}_{o}} = \exp\left[0.5\sigma_o^2\right] \tag{3}$$

Substituting values for $\bar{k}^{g}_{0.15}$ (2.98×10^{-13} m^2) and $\bar{k}^{g}_{1.27}$ (4.68×10^{-13} m^2) into Equation 3 we find that $\sigma_o^2 \ge 0.9$. This suggests that the point-support variance must be much larger (19 times) than that measured with the smallest tip (Table 1) to achieve a close fit between the model and data.

We now employ the restriction of non-uniform flow and investigate its effect on the predicted behavior of the mean upscaling. Permeability upscaling, under conditions of non-uniform flow, has been the subject of a series of studies. In each case this issue has only been explored within the context of theoretical modeling and/or numerical simulation. The analyses have largely been restricted to radially-convergent mean flows in heterogeneous/isotropic domains (Dagan, 1989; Neuman and Orr, 1993; Sanchez-Vila, 1997), one exception being Indelman and Abramovich (1994) who also investigated the case of spherical flow to a point sink in an infinite three-dimensional, isotropic domain. The key implication of these works is that under non-uniform flow conditions it is not possible to define a single effective permeability value that depends only on the statistical properties of the permeability field.

For non-uniform flow conditions we define the effective permeability, $\bar{k}_e$, as the homogeneous permeability value that provides, on average (ensemble mean), the same discharge as the heterogeneous formation under the same boundary conditions. There are only a few examples in the literature where permeability upscaling, subject to non-uniform flows, is treated in a manner consistent with our experiment (i.e., as $\bar{k}_e$). We examine two of these models.

Using stochastic perturbation methods Matheron (1967) formulated an expression for the $\bar{k}_e$ assuming radial flow to a well located in an isotropic domain. Ababou and Wood (1990) modified Matheron's result, treating the second-order approximation as a truncated exponential series expansion

$$\bar{k}_e = \bar{k}_o^g \exp\left\{ \frac{\sigma_o^2}{2} \left| \frac{2\left[1 + \left(\ln\left(r_w/\lambda_o\right)\right)^2\right]}{\left[\ln\left(r_c/r_w\right)\right]^2} - 1 \right| \right\} \tag{4}$$

where r_w is the well radius and r_c is the effective radius of the cone of depression. Consistent with Matheron they found that for fixed λ_o, $\bar{k}_e$ increases toward $\bar{k}_o^a$ as $r_w/\lambda_o \to 0$, and decreases and asymptotically approaches $\bar{k}_o^h$ (i.e., ensemble harmonic average of $k_o(\bar{x})$) as $r_c/\lambda_o \to \infty$. For similar flow conditions, Desbarats (1992b) modeled $\bar{k}_e$ as a weighted spatial geometric average where the log permeabilities were weighed by the inverse square of their distance from the well. He found $\bar{k}_e$ to decrease from $\bar{k}_o^a$ toward $\bar{k}_o^g$ as the field size becomes large compared to λ_o. According to these models, which assume non-uniform flow, the mean permeability should follow a decreasing trend as the sample support increases relative to λ_o. Although the difference between their assumed flow geometry (radial) and the actual flow conditions beneath the minipermeameter tip seal (approximately hemispherical) will influence the behavior of the mean upscaling, it should not effect the sense (decreasing) of the trend. Beyond predicting a decreasing trend for the mean upscaling, these models also predict that the absolute change in the mean permeability will be relatively small. According to these models the maximum change the mean could experience is bound by $\bar{k}_o^a$ and $\bar{k}_o^h$. Although we do not have data to calculate $\bar{k}_o^a$ or $\bar{k}_o^h$ we do know $\bar{k}_{0.15}^a/\bar{k}_{0.15}^h = 1.05$, which is much smaller than the measured change in the mean permeability (i.e., $k_{0.15}^a/k_{1.27}^a = 1.54$).

Discussion

A theoretical model for uniform flow in an infinite anisotropic medium predicts that the mean permeability remains constant (arithmetic average) as the sample support increases, while theoretical models for radial flow in an isotropic medium predict that the mean permeability should decrease as the sample support becomes large compared to λ_o. In contrast, the measured mean upscaling follows a deliberate, increasing trend. More important, the measured change in the mean far exceeds that theoretically anticipated for a medium with such low variance. Reasons for the discrepancy between the models and data lie in the experimental violation of assumptions on which the theoretical models are predicated. We now explore some of these assumptions in efforts to interpret the controls on the permeability upscaling measured on the Berea Sandstone.

One possible cause for the increasing mean permeability, which is not represented in the models, is that the depth and lateral dimensions of the sampling domain increases as the tip seal size increases. What if the permeability of the Berea Sandstone sample were to increase with depth into the block (i.e., normal to Face 3)? As the tip seal size is increased measurements penetrate deeper into the rock accessing zones of higher permeability, thus causing the mean permeability to increase with increasing sample support. However, this explanation seems unlikely given that all six faces of the Berea Sandstone yield a strongly increasing trend in the mean with increasing tip seal size. Similar arguments can be made concerning the increasing lateral dimensions of the sampling domain. The permeability at points around the perimeter of the sampling grid could increase with tip seal size due to increased accessibility of high permeability zones or due to increased interaction with the boundaries of the rock block. Again, this does not explain the measured upscaling as the perimeter nodes can be excluded from the larger tip seal data sets with imperceptible effect on the calculated statistics.

Another potential cause for the poor fit between the data and models may be the limited size of the sampling domain with respect to the correlation length scales characterizing the Berea Sandstone sample (i.e., lack an infinite medium, see Figure 4). The limited domain size could bias the sample means associated with the different tip seals; however, because each data set is equally subject to the same bias (since each is measured on the same grid) this effect does not explain the difference between the model and the data.

It could be argued that the measured upscaling is the result of discrete high-permeability pathways (the presence of which would violate key assumptions of the models) that are widely distributed across the rock face. That is, measurements made with the larger tip seals more often sample the high-permeability features leading to an increasing mean. Inspection of the sampled rock face and permeability maps (Figure 1) suggests the presence of such pathways oriented along select laminae. We expect the anisotropic structure of the rock, which gives rise to the spatially continuous "high" permeability pathways, to play an important role in the measured permeability upscaling; however, we currently do not feel that the anisotropy alone explains the upscaling. We support this opinion with three pieces of evidence. First, the mean permeability for the 1.27 cm tip seal is larger than 96% (all but 23 values) of the permeability values measured with the 0.31 cm tip seal, thus there are not enough "high" permeability values to explain the measured upscaling. Considering that the 0.31 cm tip seal provides full coverage of the sampling domain, using the conservative criteria that $r_{eff} = r_o$, it is very unlikely that we simply failed to sample such pathways. Second, indicator semivariograms (e.g., Deutsch and Journel, 1997) calculated from the measured permeability data sets do not support this explanation. Indicator semivariograms were calculated using cutoff values corresponding to the 10th, 25th, 50th, 75th, and 90th percentiles of the permeability distribution. Results do not reveal any discernible differences in the range values fitted to the indicator semivariograms calculated for the different permeability classes. Third, the calculated spatial weighting (filter) functions in Tidwell et al. (1999) did not discern significant anisotropy that would be diagnostic of preferred flow paths along the laminae.

These models, as well as most competing theory, assume that there exists a point-support permeability that is homogeneous, isotropic, and independent of its conditions of measurement. However, the point-support, which is associated with a fictitious, infinitely small sample support, is not a measurable quantity. In practice the local support (i.e., smallest sample support for which permeability data are available) is taken to represent the point support, sometimes subject to minor modifications (e.g., Clark, 1977). However, under non-uniform flow conditions and where heterogeneity occurs on the scale of the measurement, such treatment can be dangerous. Consider the divergent flow geometry (Figure 6) associated with a minipermeameter tip seal measurement. Now, superimpose the sample support associated with a smaller tip seal (i.e., a local support) on the flow field. If the local support is centered on the larger measurement then the local support will principally experience uniform one-dimensional flow oriented vertically into the rock surface. If the local support is moved to a position under the rubber seal, gas flow will be predominately radial and oriented parallel to the rock surface. Finally, if the local support is moved well away from the outer perimeter of the rubber seal, gas flow will again be nearly uniform and one-dimensional but oriented toward the surface of the rock. In each of these three cases the local support experiences a very different gas flow geometry depending on its position in the larger flow field. More importantly, these geometries are very different from the divergent flow geometry under which the local support is measured. Where anisotropy occurs on the scale of the local support, the permeabilities will differ depending on the dimensionality of the gas flow and its orientation with respect to the anisotropy. Evidence for such anisotropy in the Berea Sandstone is expressed in the semivariogram transects (Figure 4) calculated for each tip seal data set.

From these arguments we conclude that the primary factors influencing the upscaling measured on the Berea Sandstone sample are the non-uniform flow imposed by the minipermeameter coupled with permeability anisotropy, which occurs at scales comparable to that of the measurements. The poor fit between the data and the theoretical models results largely from the fact that our local-support permeability data, which we are forced to adopt as point-support, are inconsistent with the conditions assumed in the models; specifically, in the models the point-support permeability is isotropic and independent of its measurement conditions. We recognize that a rigorous, quantitative analysis of these coupled effects is needed; however, much effort will be required to develop the analytical and/or numerical tools with which to analyze the upscaling of non-uniform flows subject to locally-heterogeneous, anisotropic permeability distributions.

A key implication of this work is that local-support permeability values are not a intrinsic characteristic of the porous medium from which they are measured. Where non-uniform flows are an issue and/or the scale of heterogeneity approaches that of the sample support, explicit consideration of the measurement characteristics and/or media characteristics may be required in defining the point-support permeability from local-support values. These local-scale effects can have significant influence on the mean upscaling as evidenced by the comparisons drawn here. As computational capabilities continue to improve the desire to incorporate finer-scale detail into geologic simulations will follow. Thus, as the gap between the local scale and the desired scale of analysis is narrowed, precise treatment of local-scale effects will play a role of increasing importance in the modeling and upscaling of heterogeneous porous formations. However, additional work is needed to develop a proper theoretical foundation and the complimentary tools for addressing local-scale processes.

CONCLUSIONS

There are few data sets, collected under controlled experimental conditions, that clearly document the upscaling of permeability measurements collected from natural geologic materials. Here, we present the results of physical upscaling experiments performed on a block of Berea Sandstone. Using a computer automated minipermeameter test system we measured 2304 permeability values with four different sample supports (sample volumes). The data sets are unique in that measurements made at different sample supports were subject to consistent boundary conditions and flow geometries, all measurements were made on the same physical sample, and high-resolution (sub-centimeter resolution) sampling was employed at each sample support. Results show the calculated permeability statistics (i.e., permeability maps, semivariograms) to be strongly correlated with the stratified structural features visible in the sandstone sample. The summary statistics calculated from the data show clear and consistent trends with changing sample support (i.e., upscaling): among these are an increasing mean, decreasing variance, and increasing semivariogram range with increasing sample support.

To help interpret the measured upscaling we compared the observed trend in the mean permeability to predictions from two published theoretical models based, respectively, on uniform and non-uniform flow assumptions. The models significantly under predicted the measured upscaling. Discrepancies between the data and models were used to identify the basic controls on the measured permeability upscaling. We found the non-uniform flow imposed by the minipermeameter coupled with permeability anisotropy at the scale of the local support (i.e., smallest sample support for which data are available) to be the primary factors influencing the measured upscaling. The poor fit between the data and the theoretical models results largely from the fact that our local-support permeability data, which we are forced to adopt as point-support (i.e., infinitely small sample support), are inconsistent with the conditions assumed in the models; specifically, in the models the point-support permeability is isotropic and independent of its measurement conditions.

These results demonstrate both the important role of non-uniform flow on permeability upscaling and the care that must be exercised when conditioning upscaling models on local-support data. The implications of our results are not limited to minipermeameters, but rather to any instrument that imposes non-uniform flow conditions, including slug, pump, and tracer tests.

ACKNOWLEDGMENTS

We would like to thank Justin Von Doemming and Mark Bailey for help in collecting the presented data and Allan Gutjahr, Robert Glass, and Fred Phillips for providing constructive advice. We also gratefully acknowledge the helpful reviews of Sean McKenna, Peter Davies, and two anonymous reviewers. This work was supported by the U.S. Department of Energy, Office of Basic Energy Science, Geoscience Research Program, under contracts DE-AC04-94AL85000 and DE-F303-96ER14589/A000. Sandia is a multiprogram laboratory operated by Sandia Corporation, a Lockheed Martin Company, for the United States Department of Energy.

REFERENCES

Ababou, R., and Wood, E.F., 1990, Comment on "Effective groundwater model parameter values: Influence of spatial variability of hydraulic conductivity, leakance, and recharge by J.J. Gomez-Hernandez and S.M. Gorelick,": Water Resources Res., v. 26, no. 8, p. 1843-1846.

Bear, J., and Bachmat, Y., 1990, Introduction to modeling of transport phenomena in porous media: Kluwer Academic Publishers, Boston , 553 p.

Bracewell, R.N., 1986, The Fourier Transform and Its Applications: McGraw-Hill, New York, 474 p.

Clark, I., 1977, Regularization of a semi-variogram: Computers and Geosciences, v. 3, p. 341-346.

Cushman, J.H., 1984, On unifying the concepts of scale, instrumentation, and stochastics in the development of multiphase transport theory: Water Resources Res., v. 20, no. 11, p. 1668-1676.

Dagan, G., 1981, Analysis of flow through heterogeneous random aquifers by the method of embedding matrix 1. Steady flow: Water Resources Res., v. 17, no. 1, p. 107-121.

Dagan, G., 1989, Flow and Transport in Porous Formations: Springer-Verlag, New York, 465 p.

Desbarats, A.J., 1992a, Spatial averaging of hydraulic conductivity in three-dimensional heterogeneous porous media: Math. Geology, v. 24, no. 3, p. 249-267.

Desbarats, A.J., 1992b, Spatial averaging of transmissivity in heterogeneous fields with flow toward a well: Water Resources Res., v. 28, no. 3, p. 757-767.

Deutsch, C.V., and Journel, A.G., 1997, GSLIB: Geostatistical Software Library and User's Guide: Oxford University Press, New York, 368 p.

Deutsch, C.V., 1989, Calculating effective absolute permeability in sandstone/shale sequences: SPE Formation Evaluation, v. 4, no, 3, p. 343-348.

Durlofsky, L.J., 1991, Numerical calculation of equivalent grid block permeability tensors for heterogeneous porous media: Water Resources Res., v. 27, no. 5, p. 699-708.

Gelhar, L.W., and Axness, C.L., 1983, Three-dimensional stochastic analysis of macrodispersion in aquifers: Water Resources Res., v. 19, no. 1, p. 161-180.

Goggin, D. J., Thrasher, R. L., and Lake, L. W., 1988, A theoretical and experimental analysis of minipermeameter response including gas slippage and high velocity flow effects: In Situ, v. 12, no. 1-2, p. 79-116.

Gutjahr, A.L., Gelhar, L.W., Bakr, A.A., and Macmillan, J.R., 1978, Stochastic analysis of spatial variability in subsurface flows, 2. Evaluation and application: Water Resources Res., v. 14, no. 5, p. 953-960.

Indelman, P., and Abramovich, B., 1994, Nonlocal properties of nonuniform averaged flows in heterogeneous media: Water Resources Res., v. 30, no. 12, p. 3385-3393.

Journel, A G., and Huijbregts, C.J., 1978, Mining Geostatistics: Academic Press, New York, 600 p.

Kitanidis, P.K., 1990, Effective hydraulic conductivity for gradually varying flow: Water Resources Res., v. 26, no. 6, p. 1197-1208.

Kossack, C.A., Aasen, J.O., and Opdal, S.T., 1990, Scaling up heterogeneities with pseudofunctions: SPE Formation Evaluation, v. 5, no. 3, p. 226-232.

Marle, C.-M., 1967, Ecoulements monophasiques en milieu poreux: Rev. Inst. Fr. Pet., v. 22, p. 1471-1509.

Matheron, G., 1967, Elements pour une theorie des milieux poreux: Maisson et Cie, Paris, 166 p.

Neuman, S. P., 1994, Generalized scaling of permeabilities: Validation and effect of support scale: Geophys. Res. Lett., v. 21, no. 5, p. 349-353.

Neuman, S.P., and Orr, S., 1993, Prediction of steady state flow in nonuniform geologic media by conditional moments: Exact nonlocal formalism, effective conductivities, and weak approximation: Water Resources Res., v. 29, no. 2, p. 341-364.

Pepper, J.F., De Witt, W., Jr., and Demarest, D.F., 1954, Geology of the Bedford Shale and Berea Sandstone in the Appalachian Basin: U.S. Geol. Survey Prof. Paper 259, U.S. Geological Survey.

Rubin, Y., and Gomez-Hernandeż, J.J., 1990, A stochastic approach to the problem of upscaling of conductivity in disordered media: Theory and unconditional numerical simulations: Water Resources Res., v. 26, no. 4, p. 691-701.

Sanchez-Vila, X., 1997, Radially convergent flow in heterogeneous porous media: Water Resources Res., v. 33, no. 7, p. 1633-1641.

Tidwell, V.C., and Wilson, J.L., 1997, Laboratory method for investigating permeability upscaling: Water Resources Res., v. 33, no. 7, p. 1607-1616.

Tidwell, V.C., and Wilson, J.L., 1999a, Upscaling experiments conducted on a block of volcanic tuff: Results for a bimodal permeability distribution: in press Water Resources Res.

Tidwell, V.C., and Wilson, J.L., 1999b, Heterogeneity, permeability patterns, and permeability upscaling: Physical characterization of a block of Massillon Sandstone exhibiting nested scales of heterogeneity: submitted to SPE Reservoir Evaluation and Engineering.

Tidwell, V.C., Gutjahr, A.L., and Wilson, J.L., 1999, What does an instrument measure? Empirical spatial weighting functions calculated from permeability data sets measured on multiple sample supports: Water Resources Res., v. 35, no. 1, p. 43-54.

White, C.D., and Horne, R.N., 1987, Computing absolute transmissivity in the presence of fine-scale heterogeneity: paper SPE 16011, presented at the SPE Symposium on Reservoir Simulation, San Antonio, Texas.

Table 1. Summary statistics for the natural-log permeability data sets measured with different size tip seals (r_i) on Face 3 of the Berea Sandstone sample.

	0.15 cm	0.31 cm	0.63 cm	1.27 cm
Mean	-28.84	-28.60	-28.41	-28.39
Median	-28.83	-28.58	-28.39	-28.38
Standard Deviation	0.21	0.15	0.11	0.072
Variance	0.046	0.021	0.012	0.0053
Kurtosis	0.18	1.08	0.67	1.88
Skewness	-0.34	-0.75	-0.70	-1.32
Range	1.22	0.94	0.63	0.37
Minimum	-29.55	-29.17	-28.78	-28.63
Maximum	-28.33	-28.23	-28.15	-28.27
Count	576	576	576	576

Table 2. Exponential model parameters fit to the semivariograms shown in Figure 4.

Tip	C_i	σ_i^2	$\bar{\lambda}_i$ (cm)	
			Parallel	Normal
0.15	0.006	0.040	19.5	0.63
0.31	0.0	0.021	22.5	1.20
0.63	0.0	0.012	27.0	2.70
1.27	0.0	0.0053	36.0	4.89

Figure Captions

Figure 1: Photograph A) of Face 3 of the Berea Sandstone sample. Also shown are the natural-log permeability fields measured with the B) 0.15, C) 0.31, D) 0.63, and E) 1.27 cm r_i tip seals on this rock face. Data were collected on a 24 by 24 point grid with 0.85 cm centers.

Figure 2: Cumulative distribution functions for the natural-log permeability data sets given in Figure 1. Each curve represents 576 permeability values.

Figure 3: Two-dimensional semivariogram calculated from the natural-log permeability data set collected with the 1.27 cm r_i tip seal on Face 3 of the Berea Sandstone sample.

Figure 4: Semivariogram transects (symbols) for the natural-log permeability data sets measured with each of the four different-size tip seals on Face 3 of the Berea Sandstone sample. Transect orientations are A) parallel and B) normal to stratification. The fitted semivariogram models (Equation 1) are given by solid lines.

Figure 5: Mean upscaling (symbols) plotted as a function of the inner tip seal radius.

Figure 6: Schematic of the gas flow field imposed by a minipermeameter measurement. Superimposed on the flow field is the sample support associated with a smaller tip seal measurement (i.e., local support). The local support is shown in three positions to demonstrate the differences in flow conditions that it experiences depending on its location within the larger measurement. The relative sizes of the two sample supports are intended to represent that of the 1.27 cm and the 0.15 cm tip seals.

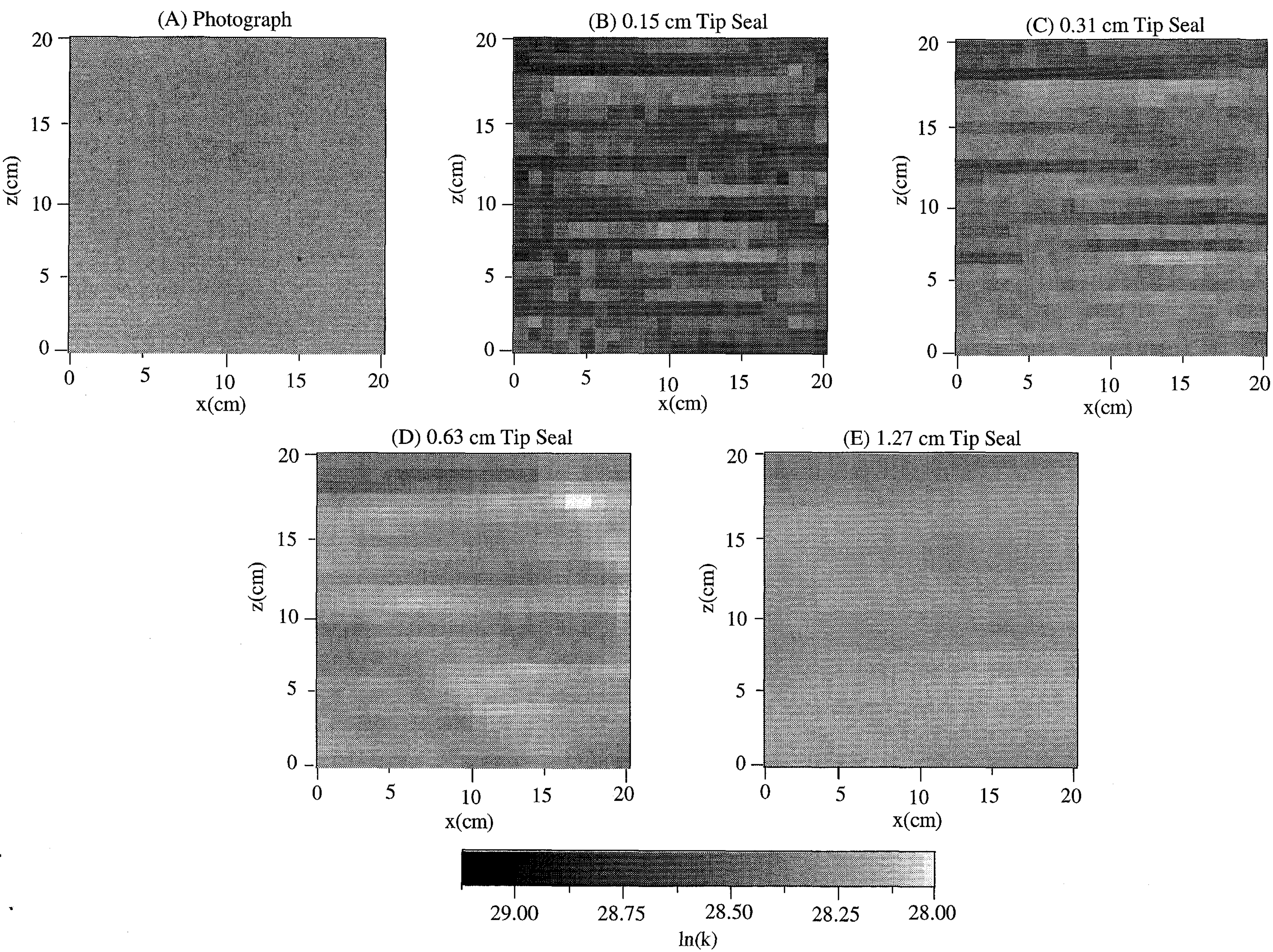
(A) Photograph
(B) 0.15 cm Tip Seal
(C) 0.31 cm Tip Seal
(D) 0.63 cm Tip Seal
(E) 1.27 cm Tip Seal
z(cm)
x(cm)
0
5
10
15
20
29.00
28.75
28.50
28.25
28.00
ln(k)

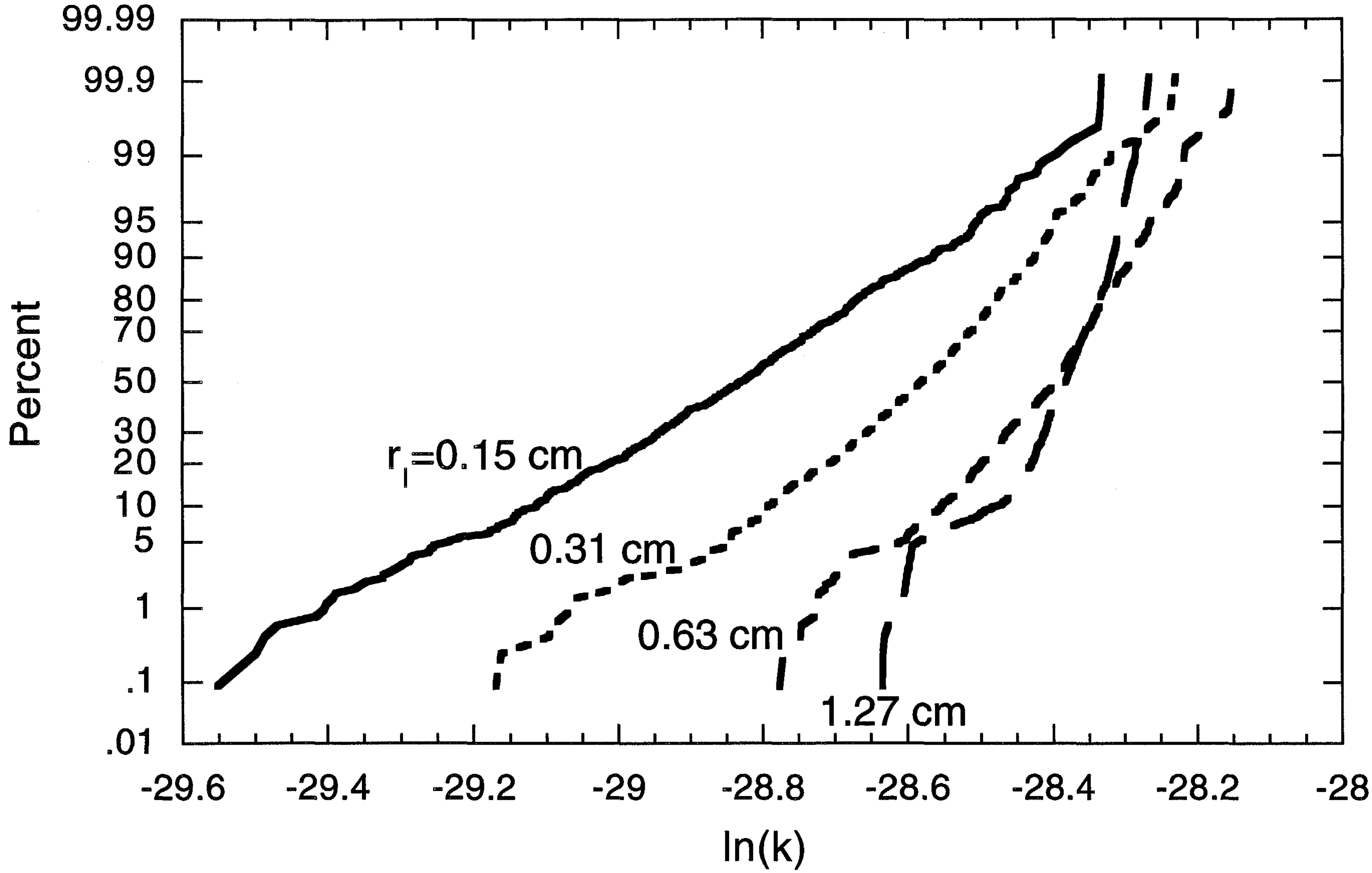

Percent
99.99
99.9
99
95
90
80
70
50
30
20
10
5
1
.1
.01
r_l=0.15 cm
0.31 cm
0.63 cm
1.27 cm
-29.6
-29.4
-29.2
-29
-28.8
-28.6
-28.4
-28.2
-28
ln(k)

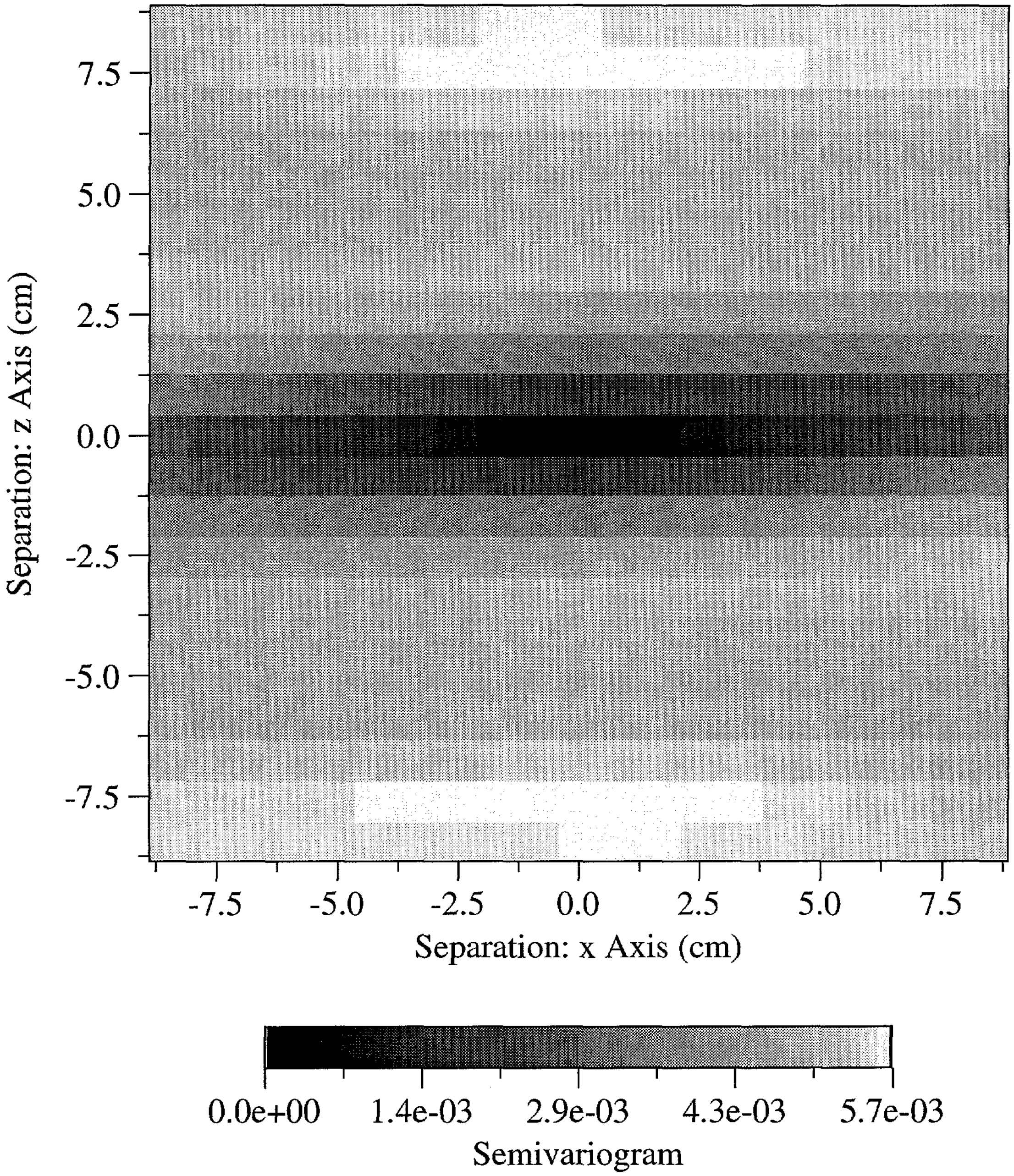
7.5
5.0
2.5
0.0
-2.5
-5.0
-7.5
Separation: z Axis (cm)
-7.5
-5.0
-2.5
0.0
2.5
5.0
7.5
Separation: x Axis (cm)
0.0e+00
1.4e-03
2.9e-03
4.3e-03
5.7e-03
Semivariogram

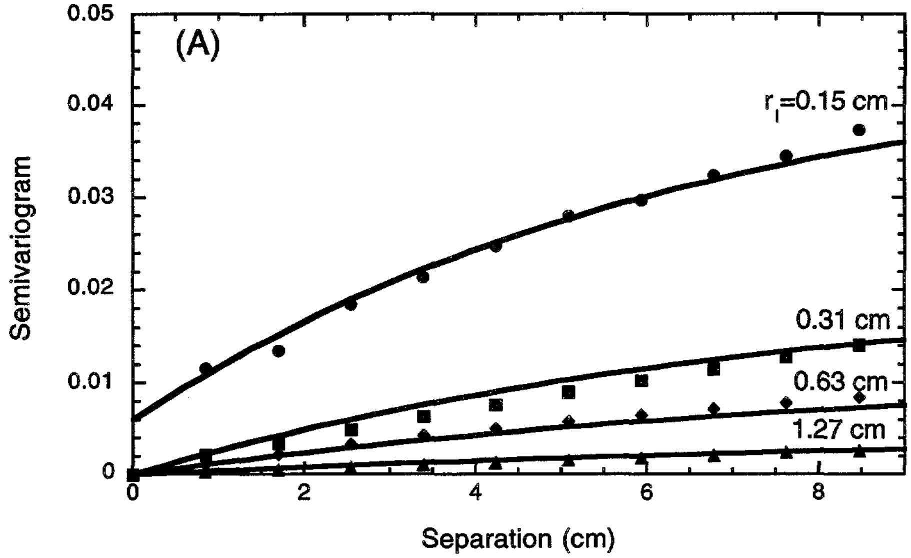
(A)
r_l=0.15 cm
0.31 cm
0.63 cm
1.27 cm
Semivariogram
Separation (cm)
0.05
0.04
0.03
0.02
0.01
0
0
2
4
6
8

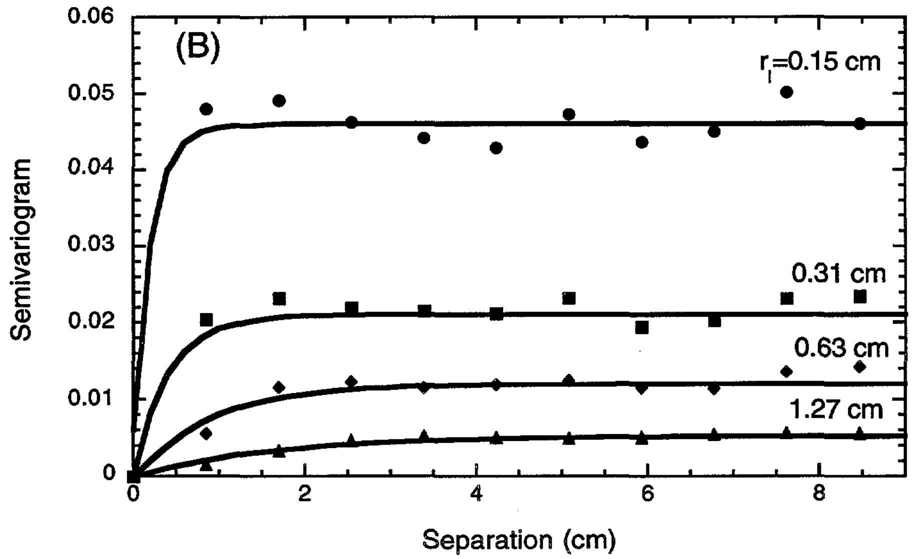
(B)
r_l=0.15 cm
0.31 cm
0.63 cm
1.27 cm
Semivariogram
Separation (cm)
0.06
0.05
0.04
0.03
0.02
0.01
0
0
2
4
6
8

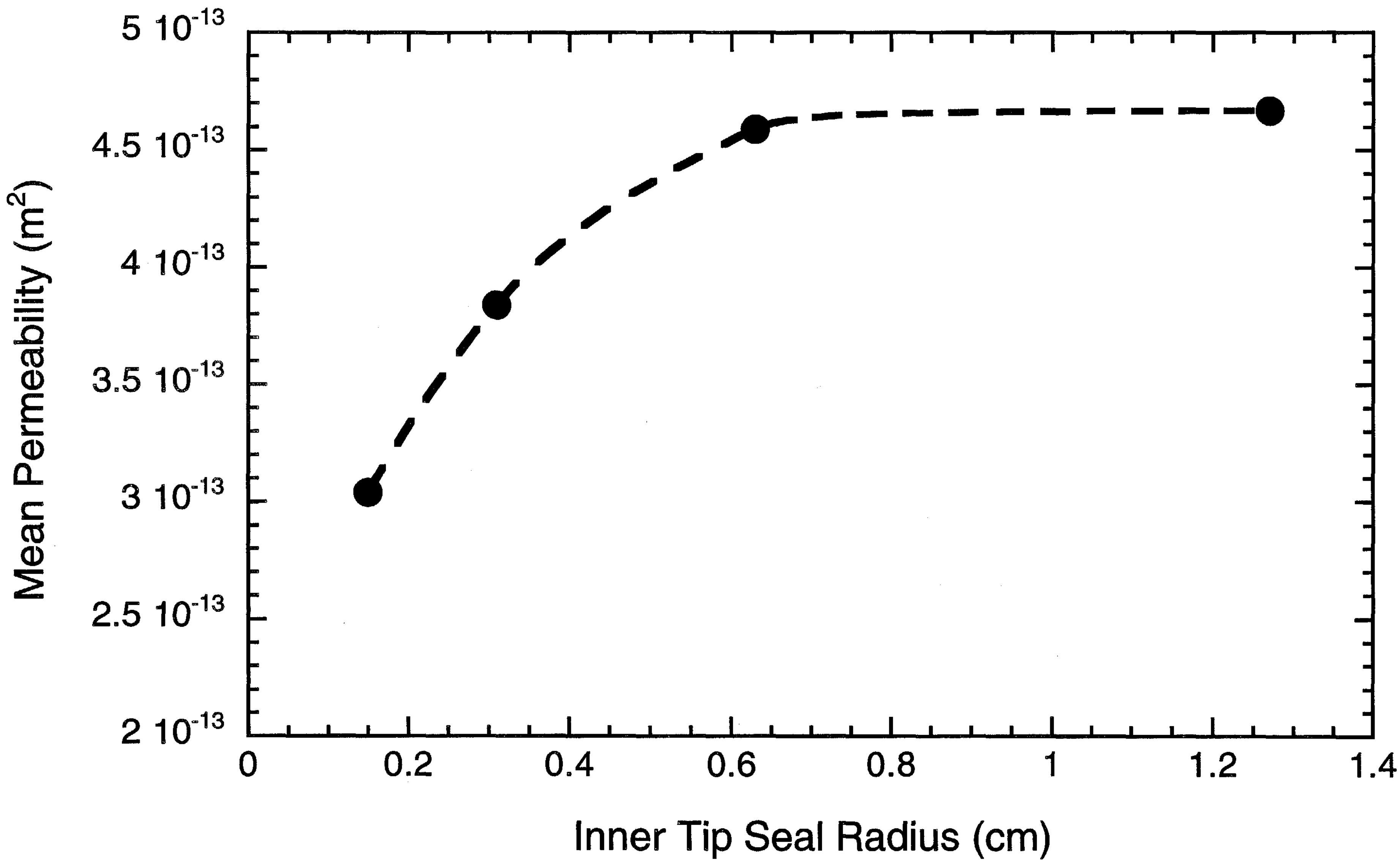
Mean Permeability (m2)
5 10-13
4.5 10-13
4 10-13
3.5 10-13
3 10-13
2.5 10-13
2 10-13
0
0.2
0.4
0.6
0.8
1
1.2
1.4
Inner Tip Seal Radius (cm)

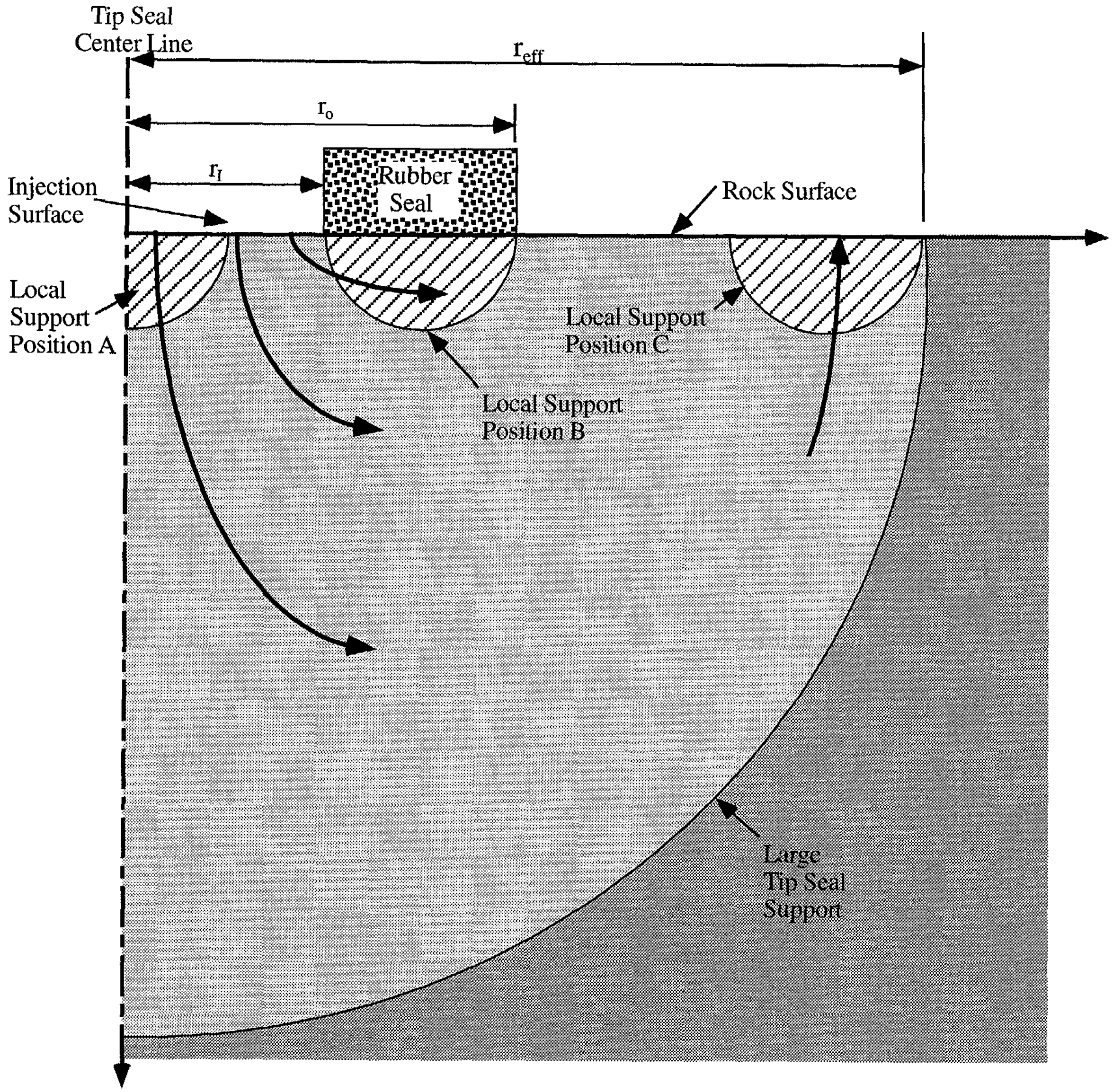
Tip Seal
Center Line
r_{eff}
r_o
r_I
Rubber
Seal
Injection
Surface
Rock Surface
Local
Support
Position A
Local Support
Position C
Local Support
Position B
Large
Tip Seal
Support